

Elena Rybalova, Eckehard Schöll, Galina Strelkova

Controlling chimera and solitary states by additive noise in networks of chaotic maps

Open Access via institutional repository of Technische Universität Berlin

Document type

Journal article | Accepted version

(i. e. final author-created version that incorporates referee comments and is the version accepted for publication; also known as: Author's Accepted Manuscript (AAM), Final Draft, Postprint)

This version is available at


<https://doi.org/10.14279/depositonce-17071>

Citation details

Rybalova, E., Schöll, E., & Strelkova, G. (2022). Controlling chimera and solitary states by additive noise in networks of chaotic maps. In *Journal of Difference Equations and Applications* (pp. 1–22). Informa UK Limited. <https://doi.org/10.1080/10236198.2022.2118580>.

This is an Accepted Manuscript of an article published by Taylor Francis in the *Journal of Difference Equations and Applications* on 12 Sep 2022, available at: <http://www.tandfonline.com/10.1080/10236198.2022.2118580>.

Terms of use

 This work is licensed under a Creative Commons Attribution-NonCommercial 4.0 International license: <https://creativecommons.org/licenses/by-nc/4.0/>

Controlling chimera and solitary states by additive noise in networks of chaotic maps

Elena Rybalova^a, Eckehard Schöll^{b,c,d}, Galina Strelkova^a

^aInstitute of Physics, Saratov State University, Saratov, 410012, Russia;

^bInstitut für Theoretische Physik, Technische Universität Berlin, 10623 Berlin, Germany;

^cBernstein Center for Computational Neuroscience Berlin, 10115 Berlin, Germany;

^dPotsdam Institute for Climate Impact Research, 14473 Potsdam, Germany

ARTICLE HISTORY

Compiled August 19, 2022

ABSTRACT

We study numerically the spatio-temporal dynamics of ring networks of coupled discrete-time systems in the presence of additive noise. The robustness of chimera states with respect to noise perturbations is explored for two ensembles in which the individual elements are described by either logistic maps or Henon maps in the chaotic regime. The influence of noise on the behavior of solitary states is investigated for a ring of nonlocally coupled Lozi maps. Numerical simulations are performed for a set of different noise realizations and random initial conditions to provide reliable statistical data. The type of dynamics of the considered networks is quantified by using a cross-correlation coefficient. We find that there is a finite and sufficiently wide region with respect to the coupling strength and the noise intensity where the probability of observing the chimeras and solitary states is high.

KEYWORDS

Network; nonlocal coupling; chimera states; solitary states; logistic map; Henon map; Lozi map

1. Introduction

Random fluctuations are unavoidable in real-world systems. They can appear as intrinsic noise or may come as external random perturbations. Studying system responses to noise is very important from a viewpoint of stability of operating modes, predicting and controlling the functioning of a majority of life-significant systems, such as infrastructure systems, power grids, transport networks, communication and information systems, biological, epidemiological, economic and social networks [4, 13, 14, 25, 38], etc. Numerical studies have demonstrated that besides a degrading function, noise can play a constructive role and gives rise to new dynamical behavior and induces novel spatio-temporal patterns which do not exist in networks of coupled dynamical systems without noise [2, 6, 19, 25, 31, 43, 51, 73]. The noise influence can also effectively control the operating modes and essentially improve certain properties of the system dynamics [2, 7]. Recently, the interest in the study of noise impact in real-world systems has significantly increased with the discovery of special partial synchronization patterns, such as chimera states [1, 10, 29, 45, 47, 49, 61, 63, 81] and solitary states

[8, 27, 34, 66]. A chimera state was reported for the first time for a network of nonlocally coupled identical phase oscillators [1, 29]. This peculiar spatio-temporal pattern represents an intermediate stage at a transition from complete coherence (synchronization) to fully incoherent (spatio-temporal chaos) dynamics and denotes the coexistence of spatially localized domains with coherent (synchronized) and incoherent (desynchronized) dynamics of network oscillators. Recent theoretical and numerical studies have demonstrated that chimera states can emerge in networks with various types of local dynamics and a variety of topologies [1, 10, 29, 45, 48, 49, 58, 60, 67, 72, 76, 82]. These partial synchronization patterns were also observed in a wide range of experimental systems [18, 21, 28, 30, 37, 53, 59, 75, 79]. Besides, chimera states can be linked to various processes occurring in real-world systems, for example, in neuroscience [5, 35, 62], in power-grids networks [39, 41, 78], in social systems [20, 24], etc.

Solitary states represent another important type of partial synchronization patterns and are defined as network states for which single or several elements behave differently compared with neighboring elements which can behave coherently or can be completely synchronized. As a rule, solitary nodes are typically randomly distributed over the network space and their number increases when the coupling strength between the network elements decreases. It was uncovered that the emergence of solitary states is related to the appearance of bistable individual dynamics due to nonlocal interaction [27, 34]. Recently, solitary states have been found in networks of the Kuramoto-Sakaguchi models and the Kuramoto oscillators with inertia [8, 26, 27, 34, 80], the discrete-time systems [55, 67, 68, 70], the FitzHugh–Nagumo systems [40, 54, 64, 65], models of power grids [9, 22, 74], and even in experimental setups of coupled pendula [28].

The robustness of chimera states with respect to noise was investigated in nonlocally coupled networks of discrete-time maps with Gaussian and uniformly distributed parameters [36, 42] and in the presence of additive and multiplicative noise [12, 44, 56], as well as in networks of continuous-time systems [32, 46, 69, 83]. In particular, it has been demonstrated that noise can induce the appearance of novel chimera patterns, such as coherence-resonance chimeras in a ring network of FitzHugh–Nagumo neurons [69], or new spatio-temporal patterns, e.g., solitary states and solitary state chimeras in a network of nonlocally coupled Henon maps [11, 57]. The dependence of the chimera lifetime on the noise was studied in nonlocally coupled networks of periodic and chaotic oscillators [32, 56, 71, 83]. It was shown that amplitude chimeras are long-living transients and can be controlled by noise influence. The noise permits to decrease the lifetime of amplitude chimeras in a ring network of Stuart–Landau oscillators [32, 83] and to increase it to infinity in ensembles of nonlocally coupled chaotic oscillators [56, 71]. Nevertheless, it is still not completely understood how the probability of observing chimera states in networks of nonlocally coupled chaotic oscillators depends on the additive noise intensity, the coupling strength, and random initial conditions.

In contrast to the analysis of chimera states in the presence of noise, the robustness of solitary states with respect to noise has not been elucidated at all until very recently, except [17], where it was shown that the presence of noise in a ring of nonlocally coupled FitzHugh–Nagumo oscillators leads to a transition from solitary states to patched synchrony. Thus, a more detailed study is needed to analyze the behavior of solitary states in the presence of external random fluctuations.

In the present paper we investigate the influence of additive noise on chimera states in networks of nonlocally coupled logistic and Henon maps and on solitary states in a network of nonlocally coupled Lozi maps. We explore how the existence of these pe-

cular partial synchronization patterns depends on the coupling strength and random initial conditions in the presence of external noise. In order to provide good statistical data we use different noise realizations for each of 50 different realizations of randomly distributed initial conditions. The cross-correlation coefficient between network elements is calculated to characterize the observed spatio-temporal structures and to automatically detect and count chimera states and solitary nodes in the considered networks both without and in the presence of noise.

2. Networks under study

2.1. Model equations

In this paper we investigate numerically the spatiotemporal dynamics of a network which is represented by a ring of nonlocally coupled chaotic maps and is subjected to additive noise. The mathematical model of the network, in its general form, reads:

$$\begin{aligned} x_i(n+1) &= F_i(n) + \frac{\sigma}{2R} \sum_{j=i-R}^{i+R} [F_j(n) - F_i(n)] + D\xi_i(n), \\ y_i(n+1) &= G_i(n), \end{aligned} \quad (1)$$

where $x_i(n)$ and $y_i(n)$ are dynamical variables, $i = 1, 2, 3, \dots, N$, $N = 1000$ is the total number of elements in the ensemble, n denotes the discrete time. Functions $F_i(n)$ and $G_i(n)$ are defined by the right-hand sides of the equations of the respective map (they will be described below). The elements within the ring are coupled in a nonlocal way, i.e., each i th element is linked with R neighbors on the left and right, respectively. Parameter R denotes the coupling range and σ is the coupling strength between the elements. We choose and fix $R = 320$ for all our numerical simulations. The last term in the first equation of (1) corresponds to the influence of additive noise which is uniformly distributed within the interval $[-1, 1]$, where $\xi_i(n)$ is a noise generator, and D is the noise intensity. We have also studied the effect of additive Gaussian noise sources on the network of coupled maps. However, the obtained results have shown a qualitative similarity to the case of uniformly distributed noise.

As individual elements in the network (1), we have used the logistic map [15, 16], the Henon [23] and the Lozi [33] maps. The logistic map is the simplest one-dimensional map demonstrating chaotic dynamics with a nonhyperbolic attractor and multistability [3]. The logistic map is given as follows:

$$x^l(n+1) = F^l(n) = \alpha^l x^l(n)(1 - x^l(n)), \quad (2)$$

where $x^l(t)$ is the dynamical variable, α^l is the control (bifurcation) parameter. We fix $\alpha^l = 3.8$ which corresponds to the chaotic dynamics of individual nodes when they are uncoupled.

The two-dimensional Henon map is described by the following equations:

$$\begin{aligned} x^H(n+1) &= F^H(n) = 1 - \alpha^H (x^H(n))^2 + y^H(n), \\ y^H(n+1) &= G^H(n) = \beta^H x^H(n), \end{aligned} \quad (3)$$

where $x^H(n)$ and $y^H(n)$ are the dynamical variables, and $\alpha^H > 0$ and $\beta^H > 0$ are the

control parameters. The Henon map under high-ratio compression ($\beta^H \rightarrow 0$) reduces to the logistic map. When the parameters are changed, the Henon map undergoes a period-doubling bifurcation cascade which results in the emergence of a nonhyperbolic chaotic attractor [3]. The Henon map is also characterized by the property of multistability [3]. In our calculations, the parameters of the Henon map are fixed at $\alpha^H = 1.4$ and $\beta^H = 0.2$ which corresponds to the chaotic dynamics in each uncoupled element and prevents the trajectories from divergence to infinity when the maps are coupled in a ring. It was found [45, 47, 55, 67] that when logistic maps or Henon maps are nonlocally coupled within a ring, the transition from complete chaotic synchronization to spatio-temporal chaos is accompanied by the appearance of amplitude and phase chimera states when the coupling strength decreases.

The two-dimensional Lozi map is defined by the following system of equations:

$$\begin{aligned} x^L(n+1) &= F^L(n) = 1 - \alpha^L |x^L(n)| + y^L(n), \\ y^L(n+1) &= G^L(n) = \beta^L x^L(n), \end{aligned} \quad (4)$$

where $x^L(n)$, $y^L(n)$ are the dynamical variables, and $\alpha^L > 0$ and $\beta^L > 0$ are the control parameters. In contrast to the two aforementioned maps, the Lozi map belongs to the class of chaotic maps which can be obtained as the Poincaré section of the hyperbolic class of Lorenz-type attractors. The Lozi map exhibits a quasihyperbolic chaotic attractor [50], and there is no multistability in the system phase space. We also fix $\alpha^L = 1.4$ and $\beta^L = 0.3$ which provides the chaotic behavior of the individual maps in (1) without coupling. As was shown in Ref.[67], the ring of nonlocally coupled Lozi maps demonstrates the transition from complete coherence to incoherence through the emergence of solitary states when the coupling strength between the elements decreases. The nonlocal coupling causes the birth of bistability in the dynamics of individual Lozi maps. It was found that it is precisely the coexistence of two attracting sets (bistability) in the phase space that is the mechanism for the emergence of solitary nodes in this network [68].

Due to multistability of the considered networks not all of the initial conditions provide chimera states or solitary states with the equal number of solitary nodes. The spatio-temporal dynamics of each network is studied for 50 different realizations of randomly distributed initial states of the dynamical variables $(x_i(0), y_i(0))$, each having its own additive noise realization. The noise realizations used do not change when the coupling strength and the noise intensity are varied.

2.2. Cross-correlation coefficient

In addition to the graphical representations for tracking the changes in the network dynamics (snapshots and spatio-temporal diagrams), we calculate the cross-correlation coefficient for each element of the network [77] and then plot the spatial profile (spatial distribution) of its values along the ring. The cross-correlation coefficient is defined as follows:

$$C_{1,i} = \frac{\langle \tilde{x}_1(n) \tilde{x}_i(n) \rangle}{\sqrt{\langle (\tilde{x}_1(n))^2 \rangle \langle (\tilde{x}_i(n))^2 \rangle}}, \quad i = 2, 3, \dots, N, \quad (5)$$

where $\tilde{x} = x(n) - \langle x(n) \rangle$, $\langle x(n) \rangle$ is the averaging of the x variable over time $T = 50000$ iterations. This measure shows the degree of correlation between the first element of the ensemble and all the others, and accordingly illustrates the synchronous or correlated behavior of the ring elements. The values of $C_{1,i}$ range from -1 to $+1$, where $+1$ relates to full in-phase synchronization, and -1 corresponds to full anti-phase synchronization. $C_{1,i} = 0$ indicates the absence of correlation between the network elements. Calculation of the cross-correlation coefficient enables one to detect automatically phase chimera states and solitary states in the ensembles under study. It was found earlier [77] that an incoherent cluster of a phase chimera is characterized by irregular switchings of cross-correlation coefficient values between ≈ -1 and $\approx +1$, that indicates the anti-phase nature of the oscillations of elements in time. In the case of solitary state mode, the correlation coefficient takes the values $\approx +1$ and ≈ -0.9 .

2.3. Network dynamics without noise

We first briefly overview the peculiar spatiotemporal structures (chimeras and solitary states) in the networks of Henon maps and Lozi maps without additive noise. Figure 1 shows exemplary snapshots of the x_i variables (Fig. 1,a), spatial distributions of $C_{1,i}$ (Fig. 1,b), and spatio-temporal plots of $x_i(n)$ (Fig. 1,c) for the chimera state in the ensemble of nonlocally coupled Henon maps (Fig. 1, left column) and for the solitary state in the ensemble of nonlocally coupled Lozi maps (Fig. 1, right column). A chimera state observed in the ring of nonlocally coupled logistic maps is similar to that in the Henon map ring (Fig. 1, left column).

The chimera state chosen in our simulation and shown in Fig. 1,a-c,I represents the coexistence of a phase chimera (two incoherent clusters with elements $25 < i < 55$ and $652 < i < 727$), an amplitude chimera (the incoherent cluster includes elements $300 < i < 420$), and a solitary state chimera (the incoherent cluster with nodes $877 < i < 950$). As can be seen from Fig. 1,b,I, the cross-correlation coefficient values tend to 1 or -1 for the oscillators belonging to the coherent clusters, the clusters of the phase chimera and of the solitary state chimera, while they lie within the interval $C_{1,i} \in [-1, -0.8]$ for the amplitude chimera cluster (or $C_{1,i} \in [0.8, 1]$ if the first element relative to which the cross-correlation coefficients are calculated belongs to the amplitude chimera cluster, for example $i = 100$). To automatically detect phase chimeras we take into account the fact that there are clusters where the cross-correlation coefficient changes from -1 to 1 several times (inside the incoherent cluster of phase chimeras), and clusters in which $C_{1,i}$ approaches only either -1 or 1 for all the oscillators in the coherent clusters. However, introducing the additive noise violates the ideal picture that $C_{1,i}$ is confined to values 1 and -1 . Therefore, we must define the confidence intervals $[-1, -0.8]$ and $[0.8, 1]$ instead of -1 and 1 , respectively. For the same reason, since it is rather difficult to automatically detect the amplitude chimera in a noisy ensemble, we do not determine its presence. Here, we did not distinguish between the phase chimeras and the solitary state chimeras, since they are similar in the spatial distributions of $C_{1,i}$.

In the case of solitary states (Fig. 1,a-c,II), the snapshot consists of a coherent plateau (typical states) and solitary nodes evenly distributed over the entire ensemble (Fig. 1,a,II). The cross-correlation coefficients for oscillators in the typical state are equal to 1 (or -1 if the first oscillator is a solitary node), and for solitary nodes $C_{1,i} \approx -0.9$ (or 0.9 , if the first oscillator is a solitary node) (see Fig. 1,b,II). In the presence of additive noise, the absolute value of the cross-correlation coefficient

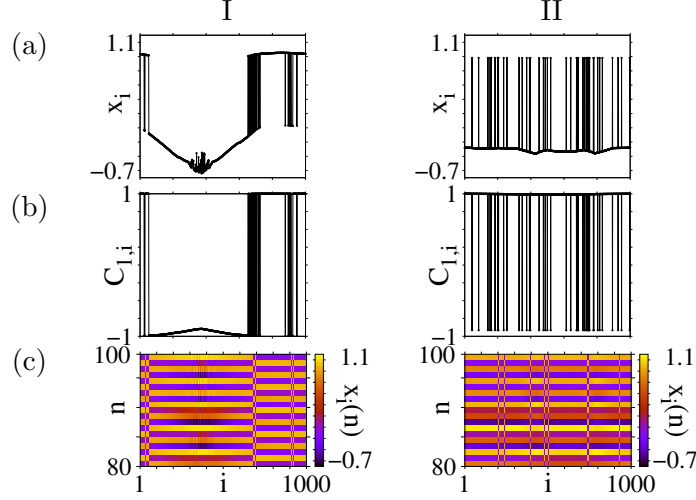


Figure 1. Examples of a combined chimera state in the Henon map ring at $\sigma = 0.275$ (panel I) and a solitary state mode in the Lozi map ring at $\sigma = 0.18$ (panel II) without noise. Snapshots of the x_i variables (a), spatial distributions of the cross-correlation coefficient (b), and spatio-temporal diagrams of $x_i(n)$ (c). Parameters: $\alpha^H = 1.4$, $\beta^H = 0.2$, $\alpha^L = 1.4$, $\beta^L = 0.3$, $R = 320$, $D = 0$, $N = 1000$

changes, as in the case of chimera states. If the first oscillator is in the typical state, the $C_{1,i}$ values lie within the interval $[-1, -0.7]$ for the solitary nodes. If the first oscillator is a solitary node, the cross-correlation coefficient for the solitary nodes takes the values from the interval $[0.7, 1]$. We have used these values to automatically find the solitary nodes.

3. Effect of additive noise on chimera states

In this section, we consider the effect of external additive noise on the spatio-temporal dynamics in the networks of nonlocally coupled chaotic maps with a nonhyperbolic chaotic attractor. As individual elements we choose the logistic map (Sec.3.1) and the Henon map (Sec.3.2). These ensembles can demonstrate different types of chimera states and we now explore their robustness to additive uniformly distributed noise sources with different intensities.

3.1. Network of nonlocally coupled logistic maps

We start with considering the dynamics of the logistic map network (1) without noise and with increasing coupling strength σ between the elements. The initial conditions for the dynamical variables $x_i(0)$ are chosen to be randomly distributed in the interval $[0, 1)$. The changes in the spatio-temporal structures of the logistic map ring are illustrated in Fig. 2 by snapshots, spatial distributions of cross-correlation coefficients and spatio-temporal diagrams. At a weak coupling strength ($0 < \sigma < 0.15$), the network shows the regime of complete spatio-temporal incoherence, which turns into spatial incoherence with periodic dynamics of the elements in time when the coupling strength increases (Fig. 2,I). When $0.25 < \sigma < 0.4$, we have some probability to obtain either the coexistence of amplitude and phase chimeras (Fig. 2,II) or only phase chimeras (Fig. 2,III). For some realizations of the initial conditions, only amplitude

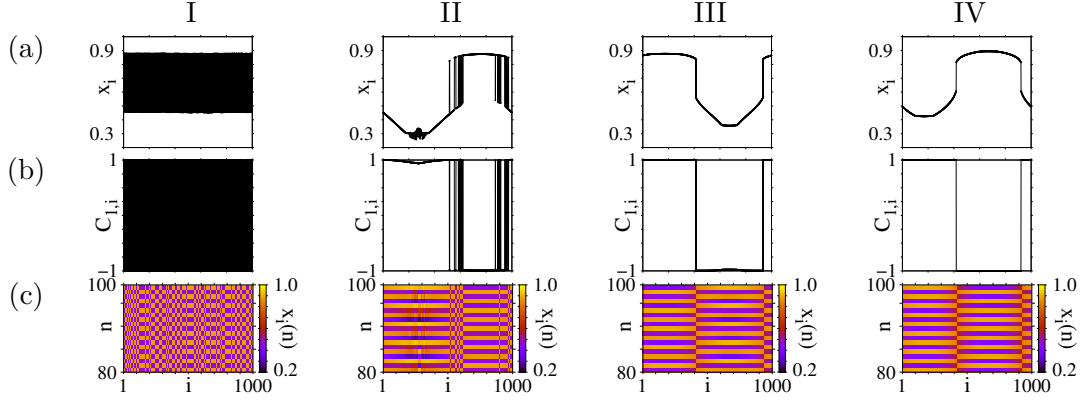


Figure 2. Dynamics of the noise-free network of nonlocally coupled logistic maps for different values of the coupling strength σ : 0.24 (panel I), 0.295 (panel II), 0.345 (panel III), 0.38 (panel IV). Snapshots of the x_i variables (a), spatial distributions of cross-correlation coefficient (b), and spatio-temporal diagrams of $x_i(n)$ (c). Parameters: $\alpha^l = 3.8$, $R = 320$, $D = 0$, $N = 1000$

chimera states occur in the ensemble, which are formed on the snapshot with profile discontinuities. As the coupling strength increases further, the incoherent clusters of phase and amplitude chimera states become narrower, and the probability of emerging amplitude chimera states decreases. It was analytically shown in Ref.[47] that chimera states in the ring of nonlocally coupled logistic maps with the control parameter $\alpha = 3.8$ occur up to the critical coupling strength $\sigma \approx 0.41$ where the spatial wave profile has two turning points with infinite slope. For larger values of σ , the spatial profile in the limit $N \rightarrow \infty$ is continuous, while for lower values it breaks at these turning points into two discontinuous branches, and the incoherent clusters are characterized by spatially uncorrelated sequences of nodes alternating randomly between these two branches. Due to the finite number of nodes in our simulations, chimera states are observed in our studies only up to $\sigma \approx 0.4$. However, for some realizations of the initial conditions, profiles with two discontinuities and without any chimera states appear at $\sigma < 0.4$ (See Fig. 2,IV). These profiles show the discontinuities but not the two coexisting stable branches, since they may be confined to a very small range of nodes, and their basins of attraction may have quite different sizes, so that for random initial conditions only one of the two branches may be predominantly reached by each node, and hence the incoherent bistable profile typical of chimera states is not observed. At $\sigma > 0.62$, the logistic map ensemble shifts to the regime of complete synchronization in space, which is characterized by chaotic behavior of the elements in time[47].

Now we add a uniformly distributed noise source to the first equation of the logistic map network (1) and analyze its effect on the network dynamics. Figure 3 presents a two-parameter diagram of regimes which shows the probability P of observing chimera states depending on the coupling strength σ and the noise intensity D . The quantity P denotes the normalized number of initial realizations $P = K/50$, where K is the number of initial sets for which chimera states arise in the network. Qualitatively, one may distinguish between the intervals of weak ($D \in [0, 0.005]$) and strong noise ($D > 0.005$).

As follows from the diagram (Fig. 3), for weak noise ($D < 0.005$), there is still a wide interval of the coupling strength σ where the chimera states are observed with a rather high probability (yellow and orange colors). With increasing noise, the probability of chimera states near the right boundary of this interval even increases because noise induces transitions between the basins of attraction of the two branches of the

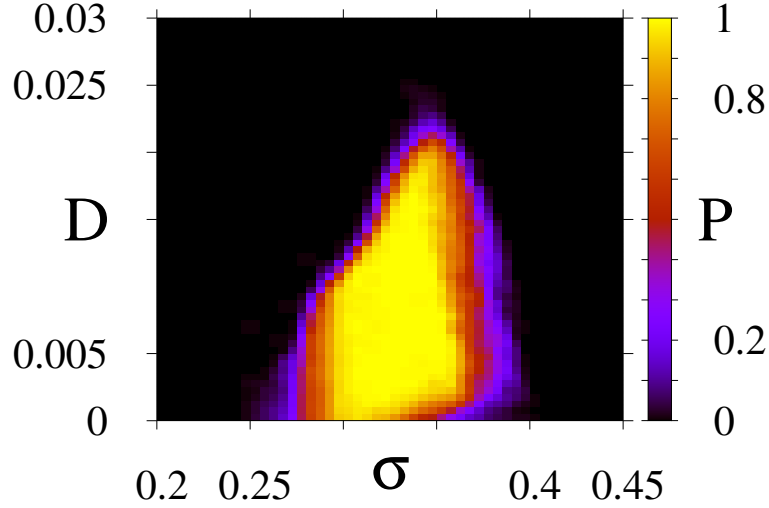


Figure 3. 2D diagram in the (σ, D) parameter plane showing the probability P of observing chimera states in the logistic map ring. Calculations were carried out for 50 different realizations of randomly distributed initial conditions, each having its own noise realization. Parameters: $\alpha^l = 3.8$, $R = 320$, $N = 1000$

profile, and thus the incoherence clusters of the phase chimera in the vicinity of the discontinuity points of the spatial profile become better visible. Figures 4,I-IV show the dynamics of the logistic map network for weak noise intensity and at the same values of σ as in the noise-free case (Fig. 2). It is seen that the snapshots of the noisy network dynamics (Fig. 4,I-III) are rather similar to those without noise, and only minor noise-induced fluctuations are observed on the spatial profiles. Figure 4,IV illustrates the case when in the presence of noise the incoherence clusters of the phase chimera near the discontinuity points of the snapshot are broadened (compare Fig. 2,IV without chimeras and Fig. 4,IV with the phase chimera with the incoherence cluster $895 < i < 899$). The reason for this is the noise-induced transitions between the two basins of attraction of the two branches, which broadens the incoherent clusters. This constitutes a constructive influence of noise.

In the case of strong noise influence, $D > 0.005$, the width of the chimera region is reduced markedly with respect to σ (Fig. 3). The changes in the network dynamics in the presence of strong noise are illustrated in Figs. 5,I-IV for the same values of σ as in the previous cases. When the coupling strength is very weak, the incoherent profile does not undergo qualitative changes, only small fluctuations occur in the system profile (compare Fig. 2,I and Fig. 5,I). At a weak coupling strength which is related to the observation of chimera states in the noise-free system, the noise effect destroys the whole spatial structure in the network (Fig. 5,II). Now a strongly incoherent snapshot of spatial profile corresponds to the network dynamics (Fig. 5,a,II). However, the elements still oscillate periodically in time (Fig. 5,c,II) and the cross-correlation coefficients take rather large values $C_{1,i} > 0.89$ (Fig. 5,b,II). With increasing coupling strength, a phase chimera with noisy coherent clusters is clearly observed in the logistic map ring (Fig. 5,III). Finally, when the coupling strength corresponds to a spatial profile with a discontinuity or narrow clusters of the phase chimera, additive noise smears out and "smooths" the profile (Fig. 5,a,IV), which is especially apparent on the distribution of cross-correlation coefficient values (Fig. 5,b,IV).

In summary, from Fig.3 it follows that there exists an optimum non-zero noise

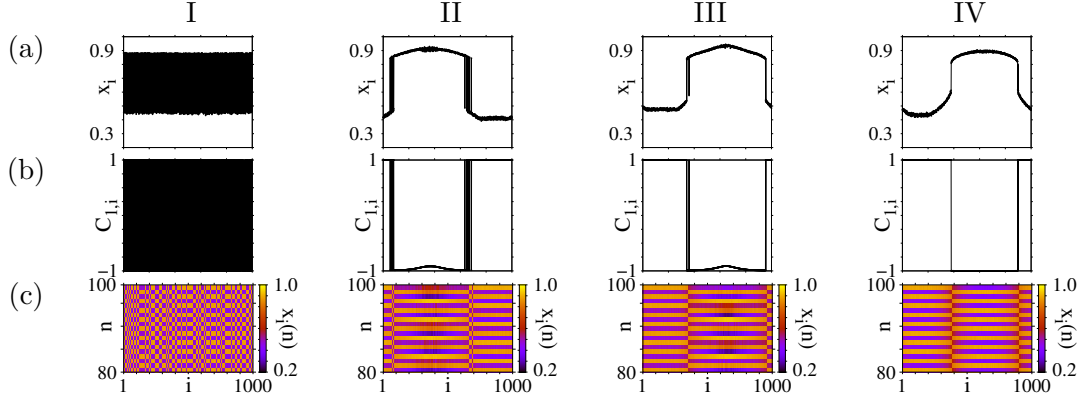


Figure 4. Dynamics of the network of nonlocally coupled logistic maps in the presence of weak noise $D = 0.0045$ and for different values of the coupling strength σ : 0.24 (panel I), 0.295 (panel II), 0.345 (panel III), 0.38 (panel IV). Snapshots of the x_i variables (a), spatial distributions of cross-correlation coefficient (b), and spatio-temporal diagrams of $x_i(n)$ (c). Parameters: $\alpha^l = 3.8$, $R = 320$, $N = 1000$

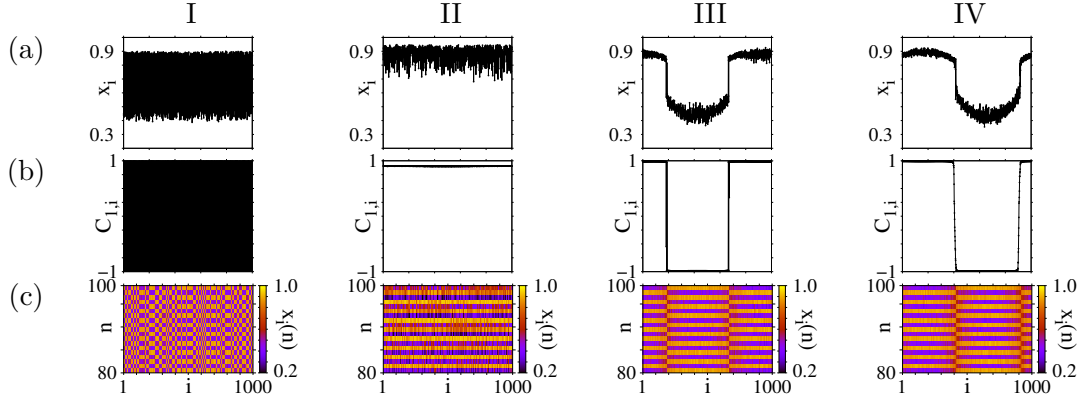


Figure 5. Dynamics of the network of nonlocally coupled logistic maps in the presence of strong noise $D = 0.02$ and for different values of the coupling strength σ : 0.24 (panel I), 0.295 (panel II), 0.345 (panel III), 0.38 (panel IV). Snapshots of the x_i variables (a), spatial distributions of cross-correlation coefficient (b), and spatio-temporal diagrams of $x_i(n)$ (c). Parameters: $\alpha^l = 3.8$, $R = 320$, $N = 1000$

intensity D where the σ -interval of chimera observation is maximum. This counter-intuitive constructive effect of noise in some sense can be treated as a resonance-like effect since the constructive and destructive action of noise are balanced for some intermediate value of the noise strength.

3.2. Network of nonlocally coupled Henon maps

The ring of nonlocally coupled Henon maps can demonstrate phase and amplitude chimeras within a certain range of the coupling strength [10, 67]. The introduction of multiplicative noise into this ensemble can induce the appearance of a solitary state chimera [57], which is characterized by the presence of an incoherent cluster containing only solitary nodes. This type of chimera can also be observed in the Henon map ensemble without external noise, but its basin of attraction is small and is unlikely observed for random initial conditions.

As before, we first briefly consider the spatio-temporal dynamics of the noise-free

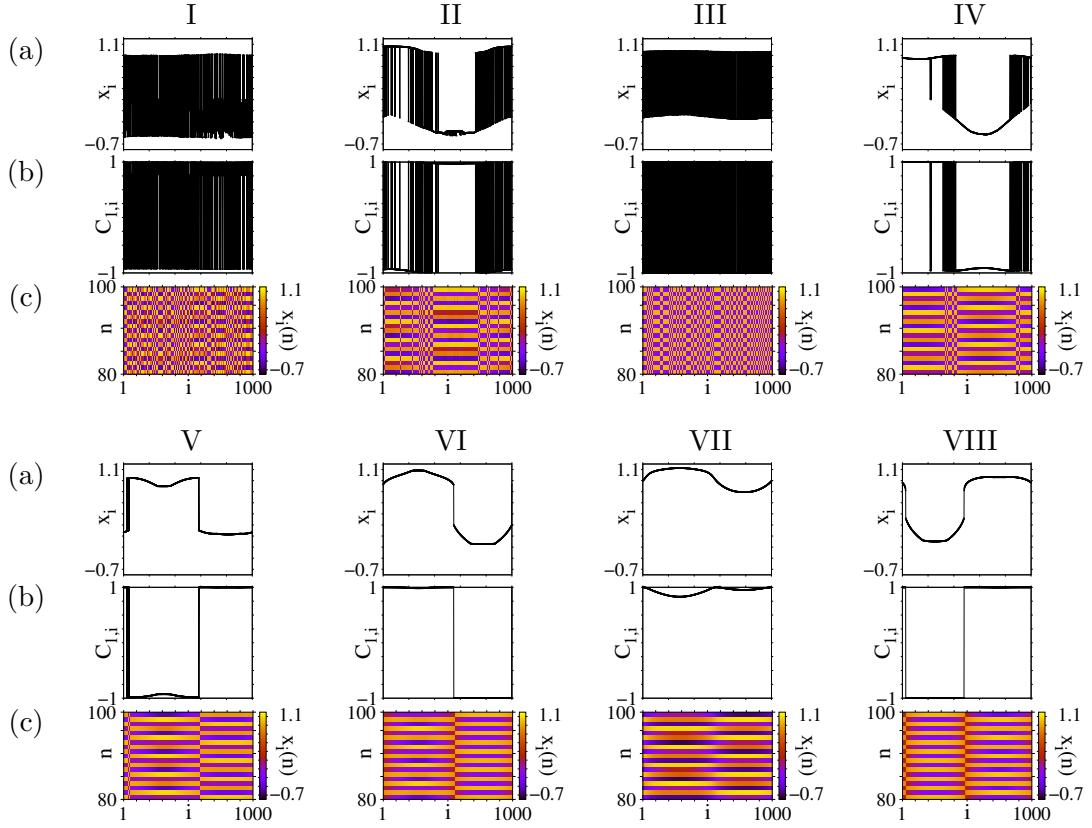


Figure 6. Dynamics of the noise-free network of nonlocally coupled Henon maps for different values of the coupling strength σ : 0.135 (panel I), 0.190 (panel II), 0.230 (panel III), 0.255 (panel IV), 0.290 (panel V), 0.380 (panel VI), 0.395 (panel VII), 0.405 (panel VIII). Snapshots of the x_i variables (a), spatial distributions of cross-correlation coefficient (b), and spatio-temporal diagrams of $x_i(n)$ (c). Parameters: $\alpha^H = 1.4$, $\beta^H = 0.2$, $R = 320$, $D = 0$, $N = 1000$

Henon map ring when the coupling strength increases. The initial conditions of the dynamical variables for all the elements $x_i(0)$, $y_i(0)$ are randomly distributed in the intervals $x_i(0) \in [-0.5, 0.5]$ and $y_i(0) \in [-0.15, 0.15]$. Figure 6 illustrates the changes in the spatio-temporal dynamics of the ring of nonlocally coupled Henon maps for selected increasing values of σ . In each of the eight panels, the upper row (a) includes snapshots of the variables x_i , the middle one (b) shows spatial distributions of cross-correlation coefficient (5), and spatio-temporal diagrams of $x_i(n)$ are given in the bottom row (c). In the case of weak coupling, a dynamical regime is observed when the network elements behave incoherently in space and non-periodically in time (Fig. 6,I). Amplitude and phase chimera states may appear in the network when σ is varied within the range $[0.17, 0.385]$. This interval of nonlocal coupling strength was established on the base of the analysis of 50 different initial distributions of the dynamical variables. For some realizations of the initial conditions, chimeras are observed at a rather weak coupling strength, and for a number of other realizations, at a stronger one. To illustrate the dynamics of the Henon map ring, one realization of the initial conditions was chosen, which leads to chimera states only at the coupling strengths corresponding to Figs. 6,II,IV,V. Figure 6,II shows the coexistence of a phase chimera (incoherent clusters with elements $1 < i < 131$, $196 < i < 428$, $717 < i < 1000$) and an amplitude chimera (the incoherent cluster includes elements $480 < i < 630$). As the coupling strength grows, it is possible to observe the coexistence of a phase chimera (two incoherent clusters: $315 < i < 417$ and $836 < i < 1000$) and a solitary states chimera (the incoherent cluster consists of elements $216 < i < 224$) (Fig. 6,IV) or only a phase chimera (two incoherent clusters: $24 < i < 45$, $583 < i < 587$) (Fig. 6,V). For some initial distributions of the dynamical variables, the σ -interval of chimera state existence can be interrupted, and in this case, the dynamics of the Henon map network corresponds to a completely incoherent spatial profile with periodic oscillations of the elements in time (Fig. 6,III). An increase in the coupling strength within the range of chimera existence leads to a decrease in the probability of observing amplitude chimeras and solitary state chimeras. At the same time, the width of the incoherent clusters of the phase chimeras decreases. When $\sigma > 0.36$ for the chosen initial conditions, the phase chimeras are not visible and one can observe an x_i profile with discontinuity (Fig. 6,VI), where the discontinuity decreases smoothly (branches must approach each other) with increasing coupling strength and, as a result, the profile must represent a smooth function. This behavior is similar as for the logistic map, and a similar analytical argument has been derived for the Henon map in [67]. However, at certain values of σ from the range corresponding to the establishment of a profile with discontinuity, smooth spatial profiles may appear, as shown in Fig. 6,VII, which can be replaced again by discontinuous profiles as the coupling strength increases (Fig. 6,VIII). For $\sigma > 0.41$, the profile discontinuity gradually decreases and, ultimately, the system goes into a chaotic synchronization mode (complete synchronization in space and non-periodic dynamics of elements in time). It should be noted that the jumps from discontinuous profiles to smooth ones and vice versa observed within the parameter range $\sigma \in [0.365, 0.410]$ are caused by the peculiarities of the phase space structure and are not related to using different initial conditions. This means that all the used initial condition do not lead to a gradual transition from the discontinuous profiles to the smooth ones with increasing the coupling strength unlike the case of the ring of nonlocally coupled logistic maps.

Now let us turn to the analysis of the effect of additive noise on chimera states in the ring of nonlocally coupled Henon maps. Figure 7 demonstrates the dependence of the probability of establishing chimera states from random initial distributions of

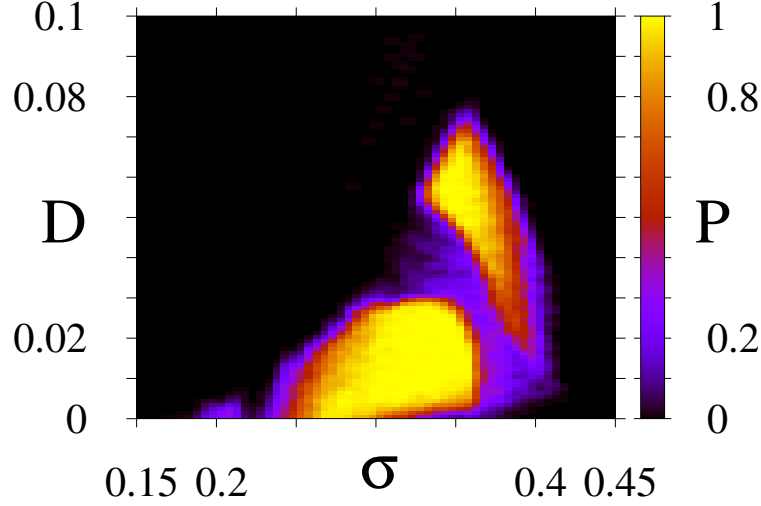


Figure 7. 2D diagram in the (σ, D) parameter plane showing the probability P of observing chimera states in the Henon map ring. Calculations were carried out for 50 different realizations of randomly distributed initial conditions, each having its own noise realization. Parameters: $\alpha^H = 1.4$, $\beta^H = 0.2$, $R = 320$, $N = 1000$

the dynamical variables on the coupling strength σ and the noise intensity D . As can be seen, when the noise intensity is low, there is a high probability of chimera state observation within a rather wide interval of the coupling strength. The maximum probability P occurs in the interval $\sigma \in [0.3, 0.35]$. However, at $D > 0.01$, a second maximum and a second region where the chimeras can be observed appear for strong coupling. These two regions are separated by a blue area, which corresponds to a low probability of observing chimeras. When $D > 0.03$, the region of chimera existence in the weak coupling range disappears, and only the second region remains. From the analysis of Fig.7 it can be concluded that the right boundary of the chimera region even shifts towards a stronger coupling with increasing noise intensity. However, we assume that this effect is rather similar to that observed in the logistic map ring. In the noise-free case when $\sigma \in [0.35, 0.42]$, the probability of chimera state observation vanishes but it can be increased by applying noise influence.

We now analyze the network behavior at a fixed noise intensity $D = 0.025$ and for different values of the coupling strength (Fig. 8). As shown above, the boundary of the chimera state region shifts to stronger coupling strength, chimera states are no longer observed at weak coupling strength, and the ensemble passes into the regime of complete spatial incoherence illustrated in Fig. 8,I. However, the cross-correlation coefficient does not vanish, i.e., the network elements demonstrate nearly periodic dynamics in time (Fig. 8,b,I). With stronger coupling, a chimera state can appear in the network even in the presence of noise with $D = 0.025$, but the width of the incoherent domain is larger than in the noise-free case (Fig. 8,II). Upon further increase of σ , the probability of observing chimera states decreases, and the network dynamics is typically characterized by a spatial wave profile with fluctuations due to noise perturbations (Fig. 8,III). For even larger values of the coupling strength, we again find a region of chimera existence. In the neighborhood of the discontinuity narrow regions of incoherence occur which correspond to incoherent clusters of the phase chimera (Fig. 8,IV).

We now fix the coupling strength $\sigma = 0.355$ and increase the noise intensity. The

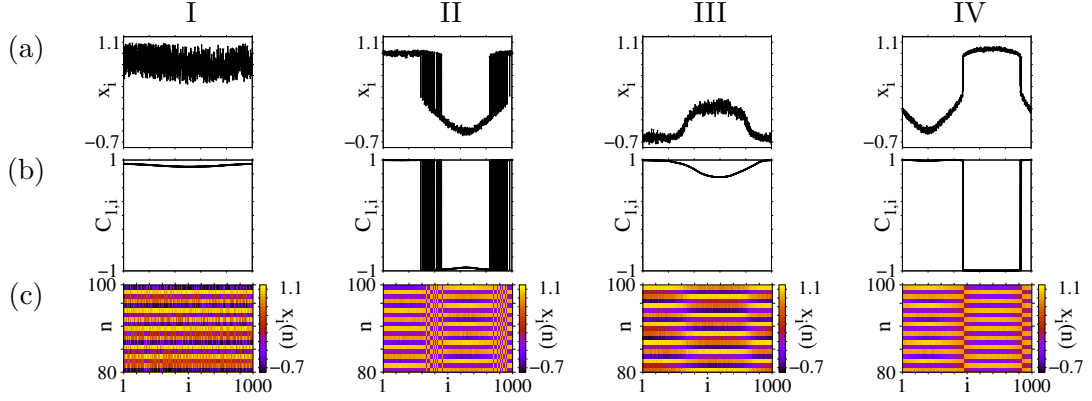


Figure 8. Snapshots of the x_i variables (a), spatial distributions of cross-correlation coefficient (b), and spatio-temporal diagrams of $x_i(n)$ (c) for the Henon map network for a fixed noise intensity $D = 0.025$ and for different values of the coupling strength σ : 0.255 (panel I), 0.285 (panel II), 0.36 (panel III), and 0.38 (panel IV). Other parameters: $\alpha^H = 1.4$, $\beta^H = 0.2$, $R = 320$, $N = 1000$

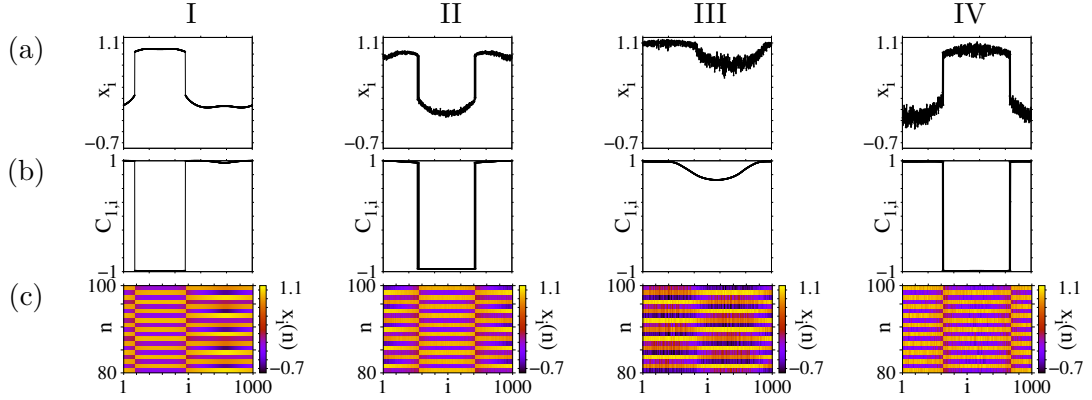


Figure 9. Snapshots of the x_i variables (a), spatial distributions of cross-correlation coefficient (b), and spatio-temporal diagrams of $x_i(n)$ (c) for the Henon map network for a fixed coupling strength $\sigma = 0.355$ and for different noise intensities D : 0 (panel I), 0.02 (panel II), 0.04 (panel III), 0.06 (panel IV). Other parameters: $\alpha^H = 1.4$, $\beta^H = 0.2$, $R = 320$, $N = 1000$

corresponding changes in the network dynamics are shown in Fig. 9. The chosen value of the coupling strength corresponds to a snapshot with two discontinuities in the noise-free case (Fig. 9,I), and the probability of observing a chimera state is extremely small (see Fig. 7). When the noise intensity is low, a phase chimera with narrow incoherent clusters appears (Fig. 9,II). Increasing the noise intensity leads to the disappearance of discontinuities in the spatial profile, and, accordingly, to the absence of chimera states (Fig. 9,III). This case corresponds to the region with a low probability of detecting chimera states (Fig. 7). When the noise intensity increases, we enter into the second region with a high probability of chimera existence, and the spatial profile contains narrow clusters of incoherence of the phase chimera (Fig. 9,IV).

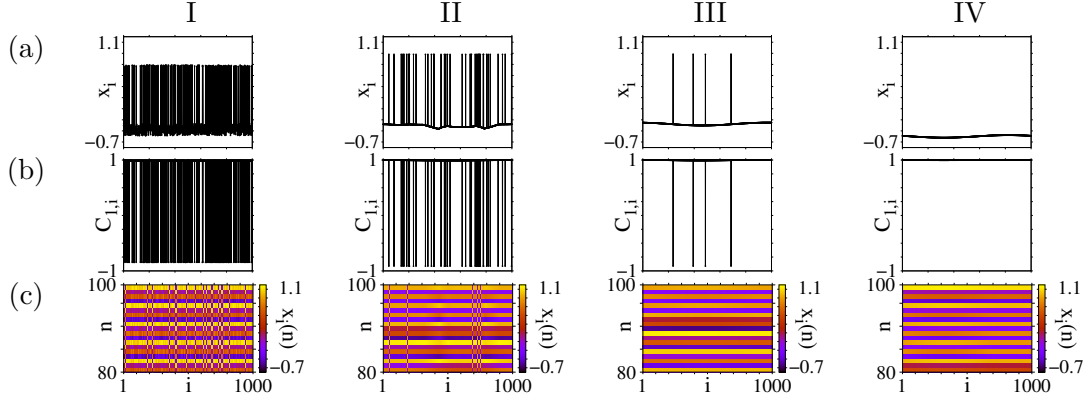


Figure 10. Dynamics of the noise-free network of nonlocally coupled Lozi maps for different values of the coupling strength σ : 0.1 (panel I), 0.18 (panel II), 0.22 (panel III), 0.24 (panel IV). Snapshots of the x_i variables (a), spatial distributions of cross-correlation coefficient (b), and spatio-temporal diagrams of $x_i(n)$ (c). Other parameters: $\alpha^L = 1.4$, $\beta^L = 0.3$, $R = 320$, $D = 0$, $N = 1000$

4. Influence of additive noise on solitary states in the ring of nonlocally coupled Lozi maps

In this section we investigate the robustness of solitary states in a ring of nonlocally coupled Lozi maps with respect to additive noise and analyze their existence depending on the noise intensity and the coupling strength. The initial conditions of all the dynamical variables in the Lozi map ring are randomly distributed in the intervals $x_i(0) \in [-0.5, 0.5]$ and $y_i(0) \in [-0.5, 0.5]$.

The ring of nonlocally coupled Lozi maps without noise can demonstrate solitary states when the coupling strength σ between the elements is varied within the range $[0, 0.22]$. Figure 10 shows how the noise-free network dynamics changes with increasing coupling strength. As can be seen from Fig. 10,I, for weak coupling strength, an incoherent mode of solitary nodes is observed in the network and is characterized by a snapshot with an incoherent plateau. Increasing the coupling strength changes the spatial profile which consists now of a coherent basis with solitary nodes (Fig. 10,II,III). The number of solitary nodes gradually decreases as σ grows. Finally, for $\sigma > 0.22$, all solitary nodes disappear, and the network dynamics corresponds to a coherent spatial profile, while the elements behave irregularly in time (Fig. 10,IV). When the coupling is sufficiently strong, the network elements become completely synchronized.

We now consider the influence of a uniformly distributed additive noise source on the formation and evolution of solitary states in the Lozi map ring. The obtained numerical results are summarized in a two-parameter diagram of regimes (Fig. 11) where the number of solitary states is plotted in dependence of the coupling strength σ and the noise intensity D . The quantity N_s is calculated by averaging the normalized number of solitary nodes S over all 50 different random initial distributions, where S is the number of solitary nodes obtained for each initial realization normalized by the total number of nodes $N = 1000$. As can be seen, the distribution of S forms an arch-shaped domain with a maximum at $D \approx 0.08$ and $\sigma \approx 0.11$. Qualitatively, one may distinguish between the intervals of weak and strong noise. Weak noise corresponds to $D < 0.02$ for which the number of solitary nodes remains almost unchanged in the presence of additive noise. If $0.02 < D < 0.04$, only the right boundary of the region of solitary node existence changes in dependence on the coupling strength. The

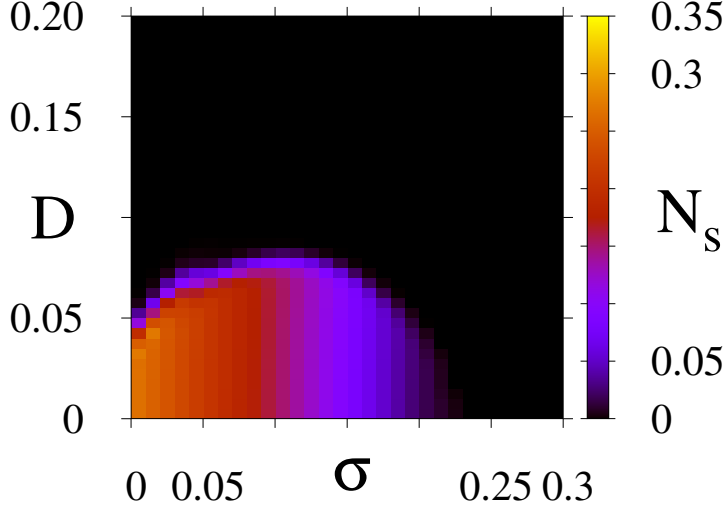


Figure 11. The average normalized number of solitary nodes N_s observed in the ring of nonlocally coupled Lozi maps in the (σ, D) parameter plane. The calculations were carried out for 50 different realizations of randomly distributed initial conditions of the dynamical variables and noise. Other parameters: $\alpha^L = 1.4$, $\beta^L = 0.3$, $R = 320$, $N = 1000$

number of solitary nodes is the largest for weak coupling strength, $0 < \sigma < 0.11$, and is gradually reduced as σ becomes stronger. When $D > 0.04$, the left boundary of the solitary state region also changes (in the region of weak coupling). In this case the additive noise is equivalent to the introduction of an inhomogeneity into the Lozi map network. This leads to the destruction of the spatio-temporal structure and to a strong inhomogeneity in the network when the cross-correlation coefficient vanishes. When the noise intensity increases, the region of solitary node existence is smoothly narrowing, while the boundaries lying both in the regions of weak and strong coupling smoothly shift to the value of $\sigma \approx 0.1$. At $D > 0.085$, the solitary states no longer exist in the Lozi map ring.

The evolution of the Lozi map dynamics is illustrated in Fig. 12 for a fixed noise intensity $D = 0.04$ and with increasing coupling strength. It is seen that at a weak coupling strength, the additive noise almost does not change the spatio-temporal structure in the ring (compare Figs. 10,I and 12,I). At a stronger coupling, the coherent basis of the spatial profile becomes noisy but the number of solitary nodes remains the same (also compare Figs. 10,II and 12,II). If the value of σ corresponds to the existence of a few solitary nodes only, then the noise intensity $D = 0.04$ is quite sufficient to reduce the basin of attraction of a solitary node attractor, and the solitary nodes are no longer observed in the network (Fig. 12,III). A further increase in the coupling strength does not cause the existing dynamical regime to qualitatively change, but leads to the increase of the cross-correlation coefficient (compare Figs. 12,III and 12,IV).

We now fix the coupling strength at $\sigma = 0.16$ and analyze the changes in the Lozi map ring dynamics as the noise intensity increases. The corresponding snapshots of the x_i variables (upper row), spatial distributions of cross-correlation coefficient values (middle row), and spatio-temporal diagrams (lower row) are shown in Fig. 13. The value of σ is chosen in such a way to observe a sufficiently large amount of solitary nodes in the network (Fig. 13,I). As noted above, the introduction of a relatively low noise intensity leads only to a noisy plateau of the spatial profile, while the solitary node number does not change in any way as compared with the noise-free case

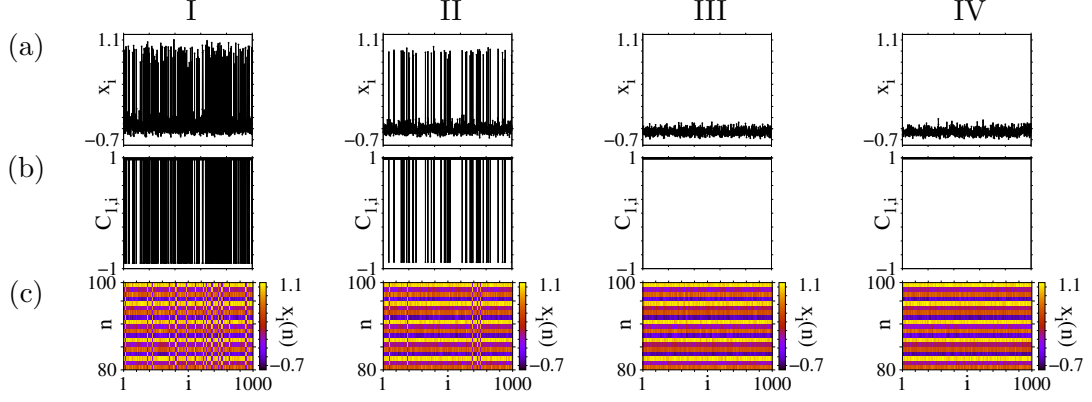


Figure 12. Snapshots of the x_i variables (a), spatial distributions of cross-correlation coefficient (b), and spatio-temporal diagrams of $x_i(n)$ (c) for the Lozi map network for a fixed noise intensity $D = 0.04$ and for different values of the coupling strength σ : 0.1 (panel I), 0.18 (panel II), 0.22 (panel III), and 0.24 (panel IV). Other parameters: $\alpha^L = 1.4$, $\beta^L = 0.3$, $R = 320$, $N = 1000$

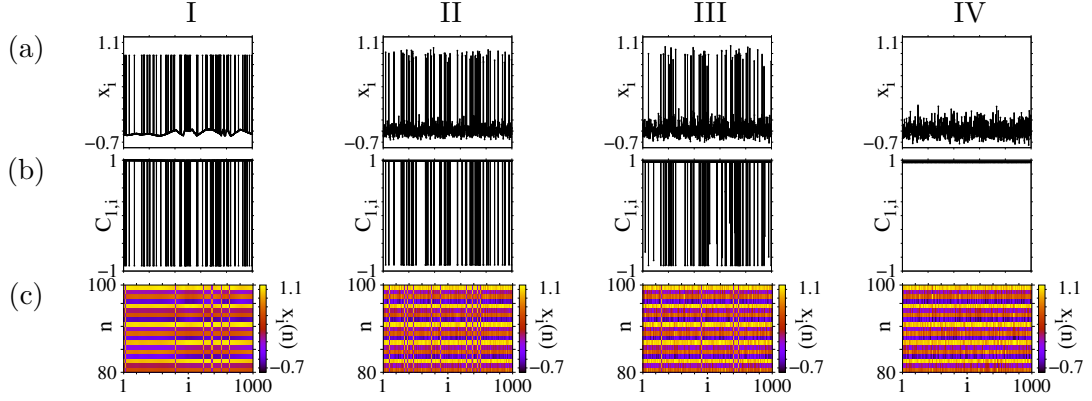


Figure 13. Snapshots of the x_i variables (a), spatial distributions of cross-correlation coefficient (b), and spatio-temporal diagrams of $x_i(n)$ (c) for the Lozi map network for a fixed coupling strength $\sigma = 0.16$ and for different noise intensities D : 0 (panel I), 0.04 (panel II), 0.065 (panel III), 0.075 (panel IV). Other parameters: $\alpha^L = 1.4$, $\beta^L = 0.3$, $R = 320$, $N = 1000$

(Fig. 13,II). When approaching the solitary state region with increasing noise intensity, the number of solitary nodes is markedly reduced since some elements jump on the attractor of typical states under the noise influence. Their cross-correlation coefficients lie within the interval $C_{1,i} \in [-0.7, 0.7]$ (Fig. 13,III). Finally, when the noise intensity is sufficiently high, the solitary state mode is destroyed and spatially incoherent dynamics is observed in the Lozi map ring (Fig. 13,IV). It should be noted that there are differences between incoherent regimes which exist for weak and strong coupling. In the first case the values of the cross-correlation coefficients of all the network elements are close to zero, while $C_{1,i} > 0.9$ in the second case.

Let us return to Fig. 13,III and pay attention to the oscillators, the cross-correlation coefficient values of which lie in the interval $C_{1,i} \in [-0.7, 0.7]$. As mentioned above, the solitary state regime is characterized by the bistable dynamics of the individual elements of the network. This means that there are two attracting sets in the phase space, one of which corresponds to the typical states or coherent dynamics (black dots in Fig. 14,c,I-III) and the other one – to the solitary nodes (red dots in Fig. 14,c,I-III). The introduction of additive noise causes some of the network oscillators to switch from the solitary node attractor to the typical state attractor (Fig. 14,II, green dots). However, their behavior is not completely synchronous with that of the typical states and thus their cross-correlation coefficient takes the values from the interval $C_{1,i} \in [-0.7, 0.7]$ (Fig. 14,b,II). For a larger noise intensity, the probability of switching between the two coexisting metastable states increases, and one can observe the solitary nodes with $C_{1,i} < -0.7$ in the network. However, they can switch between the typical state attractor and the solitary state one (blue dots in Fig. 14,c,III). Despite the fact that these oscillators were taken into account when calculating the solitary nodes, one can consider them as "imaginary" solitary nodes which belong to the typical state attractor for most of the time, but their oscillations are not synchronous with those of the coherent part $C_{1,i} < -0.7$.

5. Conclusion

In this study we have demonstrated how additive uniformly distributed noise influences the emergence and existence of special partial synchronization patterns, such as chimera states and solitary states, in networks of nonlocally coupled chaotic maps. We have studied the robustness of chimera states with respect to noise using ring networks of either logistic maps or Henon maps. It is known that these networks demonstrate a transition from complete chaotic synchronization to complete incoherence through the appearance of phase and amplitude chimeras. The effect of noise sources on solitary states has been investigated in a ring of Lozi maps with nonlocal interaction. The latter typically exhibits the existence of solitary states along the transition to spatio-temporal chaos when the coupling strength decreases.

For both cases (chimeras and solitary states) we have investigated how regions of existence of these patterns change when the nonlocal coupling strength σ and the additive noise intensity D are varied. To this purpose we have calculated the cross-correlation coefficients between network elements. Using this correlation measure we can diagnose the type of spatio-temporal dynamics of the considered networks, as well as detect phase chimeras and solitary states. In order to provide reliable statistical data we have performed numerical simulations for 50 sets of randomly distributed initial conditions each possessing its own independent noise realizations. Furthermore, we have illustrated the effects of noise on chimera and solitary states by snapshots,

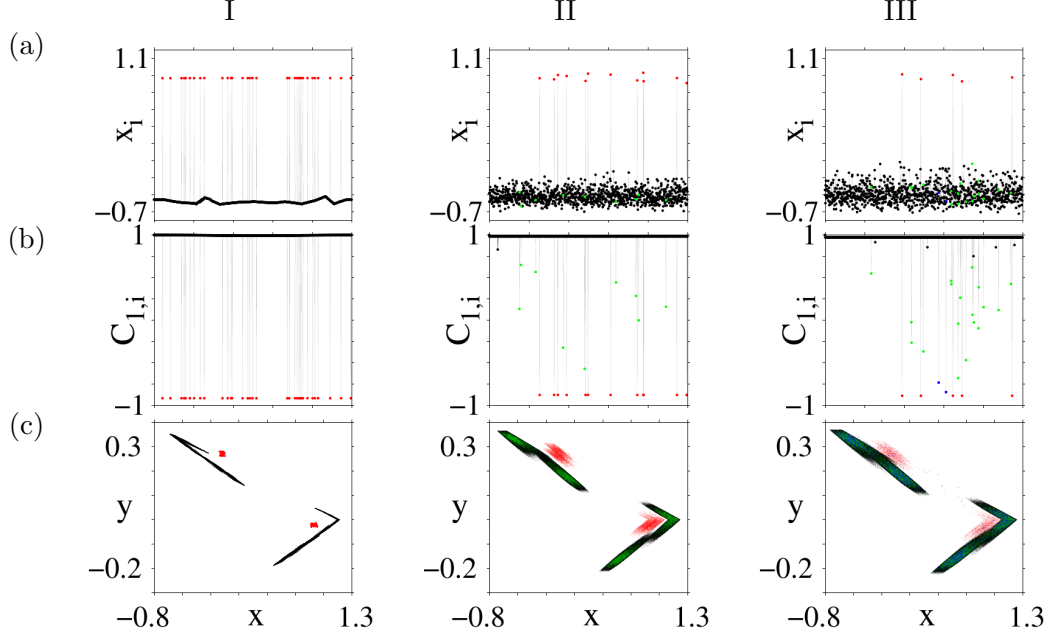


Figure 14. Snapshots of the x_i variables (a), spatial distributions of cross-correlation coefficient $C_{1,i}$ (b), and phase portraits of all elements (c) of the Lozi map for different values of the coupling strength and the noise intensity: $D = 0$, $\sigma = 0.19$ (panel I), $D = 0.05$, $\sigma = 0.19$ (panel II), $D = 0.65$, $\sigma = 0.17$ (panel III). Black points correspond to the typical states, red ones to the solitary nodes, green ones to the typical states with $C_{1,i} \in [-0.7, 0.7]$, and blue ones to oscillators which switch between the typical state attractor and the solitary state one. Other parameters: $\alpha^L = 1.4$, $\beta^L = 0.3$, $R = 320$, $N = 1000$

spatial distributions of cross-correlation coefficient values and space-time plots.

We have computed two-parameter diagrams of regimes in the (σ, D) parameter plane, which show the probability of observing chimera states in networks of coupled logistic maps and Henon maps. It has been shown that in the case of the logistic map, the phase chimeras can exist within a rather wide interval of the noise intensity and a finite range of the coupling strength, and a high probability of observing chimera states is detected for rather strong noise. In the case of the Henon map, it has been found that there are two clearly distinguished regions in the (σ, D) parameter plane, within which the phase chimera regimes persist even for rather large values of the noise intensity. However, in both networks, already very weak noise can completely suppress the chimera states in the case of weak and strong nonlocal coupling. Interestingly, we have observed a counter-intuitive non-monotonic dependence of the chimera existence upon noise intensity in both networks, which is reminiscent of the constructive influence of noise known from coherence resonance.

To analyze the robustness of solitary states in a ring network of nonlocally coupled Lozi maps with respect to additive noise we have plotted the normalized number of solitary nodes in the (σ, D) parameter plane. The main result is that even weak noise can sustain the solitary state regime in the range of weak nonlocal coupling. Stronger noise causes the solitary nodes to disappear for any values of the coupling strength. It can be assumed that this effect is related to noise-induced preference of attractors [52]. In the presence of noise, a small basin of attraction of solitary nodes becomes smeared and thus most of the system elements go to a typical attractor with a larger basin. The similar results were reported in Ref.[17] for the network of coupled FitzHugh-Nagumo neurons in the presence additive noise.

Our findings provide a detailed understanding of the stability of chimera and solitary states and open the possibility of controlling them using additive noise sources.

Disclosure statement

The authors declare that there is no potential conflict of interest.

Funding

E.R. and G.S. acknowledge financial support from the Russian Science Foundation (project No. 20-12-00119) (numerical simulation of the dynamics of the Henon and Lozi map networks). E.S. acknowledges financial support from the German Science Foundation (DFG-Projekt Nummer 429685422 and 440145547) (numerical simulation of the dynamics of the logistic map network).

References

- [1] D.M. Abrams and S.H. Strogatz, *Chimera states for coupled oscillators*, Physical review letters 93 (2004), p. 174102.
- [2] V.S. Anishchenko, A.B. Neiman, F. Moss, and L. Schimansky-Geier, *Stochastic resonance: noise-enhanced order*, Physics-Uspekhi 42 (1999), p. 7.
- [3] V.S. Anishchenko, T.E. Vadivasova, and G.I. Strelkova, *Deterministic nonlinear systems*, Springer Series in Synergetics, Springer, 2014.
- [4] L. Arnold, *Random dynamical systems*, in *Dynamical systems*, Springer (1995), pp. 1–43.
- [5] K. Bansal, J.O. Garcia, S.H. Tompson, T. Verstynen, J.M. Vettel, and S.F. Muldoon, *Cognitive chimera states in human brain networks*, Science advances 5 (2019), p. eaau8535.
- [6] I. Bashkirtseva, L. Ryashko, and H. Schurz, *Analysis of noise-induced transitions for Hopf system with additive and multiplicative random disturbances*, Chaos, Solitons & Fractals 39 (2009), pp. 72–82.
- [7] R. Benzi, A. Sutera, and A. Vulpiani, *The mechanism of stochastic resonance*, Journal of Physics A: mathematical and general 14 (1981), p. L453.
- [8] R. Berner, A. Polanska, E. Schöll, and S. Yanchuk, *Solitary states in adaptive nonlocal oscillator networks*, The European Physical Journal Special Topics 229 (2020), pp. 2183–2203.
- [9] R. Berner, S. Yanchuk, and E. Schöll, *What adaptive neuronal networks teach us about power grids*, Physical Review E 103 (2021), p. 042315.
- [10] S.A. Bogomolov, A.V. Slepnev, G.I. Strelkova, E. Schöll, and V.S. Anishchenko, *Mechanisms of appearance of amplitude and phase chimera states in ensembles of nonlocally coupled chaotic systems*, Communications in Nonlinear Science and Numerical Simulation 43 (2017), pp. 25–36.
- [11] A. Bukh, E. Rybalova, N. Semenova, G. Strelkova, and V. Anishchenko, *New type of chimera and mutual synchronization of spatiotemporal structures in two coupled ensembles of nonlocally interacting chaotic maps*, Chaos: An Interdisciplinary Journal of Nonlinear Science 27 (2017), p. 111102.
- [12] A.V. Bukh, A.V. Slepnev, V.S. Anishchenko, and T.E. Vadivasova, *Stability and noise-induced transitions in an ensemble of nonlocally coupled chaotic maps*, Regular and Chaotic Dynamics 23 (2018), pp. 325–338.
- [13] M.J. Chacron, A. Longtin, and L. Maler, *The effects of spontaneous activity, background noise, and the stimulus ensemble on information transfer in neurons*, Network: Computation in Neural Systems 14 (2003), pp. 803–824.

- [14] A. Destexhe and M. Rudolph-Lilith, *Neuronal noise*, Vol. 8, Springer Science & Business Media, 2012.
- [15] M.J. Feigenbaum, *Quantitative universality for a class of nonlinear transformations*, Journal of statistical physics 19 (1978), pp. 25–52.
- [16] M.J. Feigenbaum, *The universal metric properties of nonlinear transformations*, Journal of Statistical Physics 21 (1979), pp. 669–706.
- [17] I. Franović, S. Eydam, N. Semenova, and A. Zakharova, *Unbalanced clustering and solitary states in coupled excitable systems*, Chaos: An Interdisciplinary Journal of Nonlinear Science 32 (2022), p. 011104.
- [18] L.V. Gambuzza, A. Buscarino, S. Chessari, L. Fortuna, R. Meucci, and M. Frasca, *Experimental investigation of chimera states with quiescent and synchronous domains in coupled electronic oscillators*, Physical Review E 90 (2014), p. 032905.
- [19] L. Gammaitoni, F. Marchesoni, E. Menichella-Saetta, and S. Santucci, *Stochastic resonance in bistable systems*, Physical Review Letters 62 (1989), p. 349.
- [20] J.C. González-Avella, M.G. Cosenza, and M. San Miguel, *Localized coherence in two interacting populations of social agents*, Physica A: Statistical Mechanics and its Applications 399 (2014), pp. 24–30.
- [21] A.M. Hagerstrom, T.E. Murphy, R. Roy, P. Hövel, I. Omelchenko, and E. Schöll, *Experimental observation of chimeras in coupled-map lattices*, Nature Physics 8 (2012), pp. 658–661.
- [22] F. Hellmann, P. Schultz, P. Jaros, R. Levchenko, T. Kapitaniak, J. Kurths, and Y. Maistrenko, *Network-induced multistability through lossy coupling and exotic solitary states*, Nature communications 11 (2020), pp. 1–9.
- [23] M. Henon, *Numerical study of quadratic area-preserving mappings*, Quarterly of applied mathematics (1969), pp. 291–312.
- [24] S. Hong and Y. Chun, *Efficiency and stability in a model of wireless communication networks*, Social Choice and Welfare 34 (2010), pp. 441–454.
- [25] W. Horsthemke and R. Lefever, *Noise-induced transitions in physics, chemistry, and biology*, Noise-induced transitions: theory and applications in physics, chemistry, and biology (1984), pp. 164–200.
- [26] P. Jaros, S. Brezetsky, R. Levchenko, D. Dudkowski, T. Kapitaniak, and Y. Maistrenko, *Solitary states for coupled oscillators with inertia*, Chaos: An Interdisciplinary Journal of Nonlinear Science 28 (2018), p. 011103.
- [27] P. Jaros, Y. Maistrenko, and T. Kapitaniak, *Chimera states on the route from coherence to rotating waves*, Physical Review E 91 (2015), p. 022907.
- [28] T. Kapitaniak, P. Kuzma, J. Wojewoda, K. Czołczynski, and Y. Maistrenko, *Imperfect chimera states for coupled pendula*, Scientific reports 4 (2014), p. 6379.
- [29] Y. Kuramoto and D. Battogtokh, *Coexistence of coherence and incoherence in nonlocally coupled phase oscillators*, Nonlinear Phenomena in Complex Systems 5 (2002), pp. 380–385.
- [30] L. Larger, B. Penkovsky, and Y. Maistrenko, *Virtual chimera states for delayed-feedback systems*, Physical review letters 111 (2013), p. 054103.
- [31] B. Lindner and L. Schimansky-Geier, *Analytical approach to the stochastic FitzHugh-Nagumo system and coherence resonance*, Physical Review E 60 (1999), p. 7270.
- [32] S.A. Loos, J.C. Claussen, E. Schöll, and A. Zakharova, *Chimera patterns under the impact of noise*, Physical Review E 93 (2016), p. 012209.
- [33] R. Lozi, *Un attracteur étrange (?) du type attracteur de Hénon*, Le Journal de Physique Colloques 39 (1978), pp. C5–9.
- [34] Y. Maistrenko, B. Penkovsky, and M. Rosenblum, *Solitary state at the edge of synchrony in ensembles with attractive and repulsive interactions*, Physical Review E 89 (2014), p. 060901.
- [35] S. Majhi, B.K. Bera, D. Ghosh, and M. Perc, *Chimera states in neuronal networks: a review*, Physics of life reviews 28 (2019), pp. 100–121.
- [36] A.K. Malchow, I. Omelchenko, E. Schöll, and P. Hövel, *Robustness of chimera states in*

- nonlocally coupled networks of nonidentical logistic maps*, Physical Review E 98 (2018), p. 012217.
- [37] E.A. Martens, S. Thutupalli, A. Fourriere, and O. Hallatschek, *Chimera states in mechanical oscillator networks*, Proceedings of the National Academy of Sciences 110 (2013), pp. 10563–10567.
 - [38] M.D. McDonnell and L.M. Ward, *The benefits of noise in neural systems: bridging theory and experiment*, Nature Reviews Neuroscience 12 (2011), pp. 415–425.
 - [39] P.J. Menck, J. Heitzig, J. Kurths, and H.J. Schellnhuber, *How dead ends undermine power grid stability*, Nature communications 5 (2014), pp. 1–8.
 - [40] M. Mikhaylenko, L. Ramlow, S. Jalan, and A. Zakharova, *Weak multiplexing in neural networks: Switching between chimera and solitary states*, Chaos: An Interdisciplinary Journal of Nonlinear Science 29 (2019), p. 023122.
 - [41] A.E. Motter, S.A. Myers, M. Anghel, and T. Nishikawa, *Spontaneous synchrony in power-grid networks*, Nature Physics 9 (2013), pp. 191–197.
 - [42] V.A. Nechaev, E.V. Rybalova, and G.I. Strelkova, *Influence of parameters inhomogeneity on the existence of chimera states in a ring of nonlocally coupled maps*, Izvestiya VUZ. Applied Nonlinear Dynamics 29 (2021), pp. 943–952.
 - [43] A. Neiman, *Synchronizationlike phenomena in coupled stochastic bistable systems*, Physical Review E 49 (1994), p. 3484.
 - [44] N.N. Nikishina, E.V. Rybalova, G.I. Strelkova, and T.E. Vadivasova, *Destruction of cluster structures in an ensemble of chaotic maps with noise-modulated nonlocal coupling*, Regular and Chaotic Dynamics 27 (2022), p. (accepted).
 - [45] I. Omelchenko, Y. Maistrenko, P. Hövel, and E. Schöll, *Loss of coherence in dynamical networks: spatial chaos and chimera states*, Physical Review Letters 106 (2011), p. 234102.
 - [46] I. Omelchenko, A. Provata, J. Hizanidis, E. Schöll, and P. Hövel, *Robustness of chimera states for coupled FitzHugh-Nagumo oscillators*, Physical Review E 91 (2015), p. 022917.
 - [47] I. Omelchenko, B. Riemenschneider, P. Hövel, Y. Maistrenko, and E. Schöll, *Transition from spatial coherence to incoherence in coupled chaotic systems*, Physical Review E 85 (2012), p. 026212.
 - [48] M.J. Panaggio and D.M. Abrams, *Chimera states on a flat torus*, Physical Review Letters 110 (2013), p. 094102.
 - [49] M.J. Panaggio and D.M. Abrams, *Chimera states: coexistence of coherence and incoherence in networks of coupled oscillators*, Nonlinearity 28 (2015), p. R67.
 - [50] Y.B. Pesin, *Dynamical systems with generalized hyperbolic attractors: hyperbolic, ergodic and topological properties*, Ergodic theory and dynamical systems 12 (1992), pp. 123–151.
 - [51] A.S. Pikovsky and J. Kurths, *Coherence resonance in a noise-driven excitable system*, Physical Review Letters 78 (1997), p. 775.
 - [52] A.N. Pisarchik and U. Feudel, *Control of multistability*, Physics Reports 540 (2014), pp. 167–218.
 - [53] D.P. Rosin, D. Rontani, N.D. Haynes, E. Schöll, and D.J. Gauthier, *Transient scaling and resurgence of chimera states in networks of Boolean phase oscillators*, Physical Review E 90 (2014), p. 030902.
 - [54] E. Rybalova, V. Anishchenko, G. Strelkova, and A. Zakharova, *Solitary states and solitary state chimera in neural networks*, Chaos: An Interdisciplinary Journal of Nonlinear Science 29 (2019), p. 071106.
 - [55] E. Rybalova, N. Semenova, G. Strelkova, and V. Anishchenko, *Transition from complete synchronization to spatio-temporal chaos in coupled chaotic systems with nonhyperbolic and hyperbolic attractors*, The European Physical Journal Special Topics 226 (2017), pp. 1857–1866.
 - [56] E.V. Rybalova, D.Y. Klyushina, V.S. Anishchenko, and G.I. Strelkova, *Impact of noise on the amplitude chimera lifetime in an ensemble of nonlocally coupled chaotic maps*, Regular and Chaotic Dynamics 24 (2019), pp. 432–445.
 - [57] E. Rybalova, G. Strelkova, and V. Anishchenko, *Mechanism of realizing a solitary state chimera in a ring of nonlocally coupled chaotic maps*, Chaos, Solitons & Fractals 115

- (2018), pp. 300–305.
- [58] J. Sawicki, I. Omelchenko, A. Zakharova, and E. Schöll, *Chimera states in complex networks: interplay of fractal topology and delay*, The European Physical Journal Special Topics 226 (2017), pp. 1883–1892.
 - [59] L. Schmidt, K. Schönleber, K. Krischer, and V. García-Morales, *Coexistence of synchrony and incoherence in oscillatory media under nonlinear global coupling*, Chaos: An Interdisciplinary Journal of Nonlinear Science 24 (2014), p. 013102.
 - [60] E. Schöll, *Synchronization patterns and chimera states in complex networks: Interplay of topology and dynamics*, The European Physical Journal Special Topics 225 (2016), pp. 891–919.
 - [61] E. Schöll, *Chimeras in physics and biology: Synchronization and desynchronization of rhythms*, Nova Acta Leopoldina 425 (2021), pp. 67–95.
 - [62] E. Schöll, *Partial synchronization patterns in brain networks*, Europhysics Letters 136 (2021), p. 18001.
 - [63] E. Schöll, A. Zakharova, and R.G. Andrzejak, *Chimera States in Complex Networks*, Frontiers Media SA, 2020.
 - [64] L. Schülen, S. Ghosh, A.D. Kachhvah, A. Zakharova, and S. Jalan, *Delay engineered solitary states in complex networks*, Chaos, Solitons & Fractals 128 (2019), pp. 290–296.
 - [65] L. Schülen, D.A. Janzen, E.S. Medeiros, and A. Zakharova, *Solitary states in multiplex neural networks: Onset and vulnerability*, Chaos, Solitons & Fractals 145 (2021), p. 110670.
 - [66] V. Semenov, A. Zakharova, Y. Maistrenko, and E. Schöll, *Delayed-feedback chimera states: Forced multiclusters and stochastic resonance*, EPL (Europhysics Letters) 115 (2016), p. 10005.
 - [67] N. Semenova, A. Zakharova, E. Schöll, and V. Anishchenko, *Does hyperbolicity impede emergence of chimera states in networks of nonlocally coupled chaotic oscillators?*, EPL (Europhysics Letters) 112 (2015), p. 40002.
 - [68] N. Semenova, T. Vadivasova, and V. Anishchenko, *Mechanism of solitary state appearance in an ensemble of nonlocally coupled Lozi maps*, The European Physical Journal Special Topics 227 (2018), pp. 1173–1183.
 - [69] N. Semenova, A. Zakharova, V. Anishchenko, and E. Schöll, *Coherence-resonance chimeras in a network of excitable elements*, Physical Review Letters 117 (2016), p. 014102.
 - [70] N.I. Semenova, E.V. Rybalova, G.I. Strelkova, and V.S. Anishchenko, *“coherence–incoherence” transition in ensembles of nonlocally coupled chaotic oscillators with nonhyperbolic and hyperbolic attractors*, Regular and Chaotic Dynamics 22 (2017), pp. 148–162.
 - [71] N. Semenova, G. Strelkova, V. Anishchenko, and A. Zakharova, *Temporal intermittency and the lifetime of chimera states in ensembles of nonlocally coupled chaotic oscillators*, Chaos: An Interdisciplinary Journal of Nonlinear Science 27 (2017), p. 061102.
 - [72] S. Shima and Y. Kuramoto, *Rotating spiral waves with phase-randomized core in nonlocally coupled oscillators*, Physical Review E 69 (2004), p. 036213.
 - [73] B. Shulgin, A. Neiman, and V. Anishchenko, *Mean switching frequency locking in stochastic bistable systems driven by a periodic force*, Physical review letters 75 (1995), p. 4157.
 - [74] H. Taher, S. Olmi, and E. Schöll, *Enhancing power grid synchronization and stability through time-delayed feedback control*, Physical Review E 100 (2019), p. 062306.
 - [75] M.R. Tinsley, S. Nkomo, and K. Showalter, *Chimera and phase-cluster states in populations of coupled chemical oscillators*, Nature Physics 8 (2012), pp. 662–665.
 - [76] S. Ulonska, I. Omelchenko, A. Zakharova, and E. Schöll, *Chimera states in networks of Van der Pol oscillators with hierarchical connectivities*, Chaos: An Interdisciplinary Journal of Nonlinear Science 26 (2016), p. 094825.
 - [77] T.E. Vadivasova, G.I. Strelkova, S.A. Bogomolov, and V.S. Anishchenko, *Correlation analysis of the coherence-incoherence transition in a ring of nonlocally coupled logistic maps*, Chaos: An Interdisciplinary Journal of Nonlinear Science 26 (2016), p. 093108.
 - [78] B. Wang, H. Suzuki, and K. Aihara, *Enhancing synchronization stability in a multi-area power grid*, Scientific reports 6 (2016), pp. 1–11.

- [79] M. Wickramasinghe and I.Z. Kiss, *Spatially organized dynamical states in chemical oscillator networks: Synchronization, dynamical differentiation, and chimera patterns*, PloS one 8 (2013), p. e80586.
- [80] H. Wu and M. Dhamala, *Dynamics of Kuramoto oscillators with time-delayed positive and negative couplings*, Physical Review E 98 (2018), p. 032221.
- [81] A. Zakharova, *Chimera patterns in networks: Interplay between dynamics, structure, noise, and delay*, Springer Nature, 2020.
- [82] A. Zakharova, M. Kapeller, and E. Schöll, *Chimera death: Symmetry breaking in dynamical networks*, Physical Review Letters 112 (2014), p. 154101.
- [83] A. Zakharova, S. Loos, J. Siebert, A. Gjurchinovski, and E. Schöll, *Chimera patterns: influence of time delay and noise*, IFAC-PapersOnLine 48 (2015), pp. 7–12.